

# Enhanced CO<sub>2</sub> Capture-Desorption by Surface-Active Amine

Abdulmuiz A. Adekom, Omar A. Carrasco-Jaim,\* Upali P. Weerasooriya, and Ryosuke Okuno



Cite This: *Energy Fuels* 2024, 38, 14435–14448



Read Online

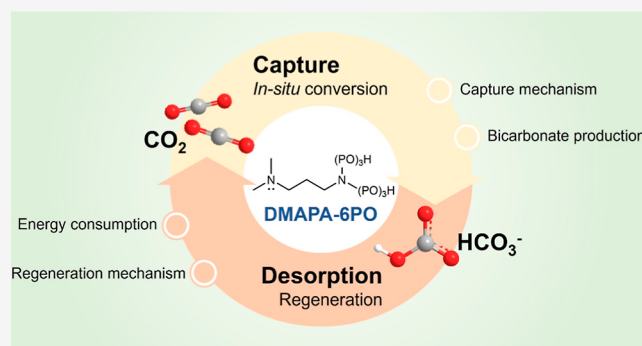
ACCESS |

Metrics & More

Article Recommendations

Supporting Information

**ABSTRACT:** Developing an efficient solvent for carbon dioxide (CO<sub>2</sub>) capture stands as a pivotal step in mitigating greenhouse gas emissions and long-term climate change. In this study, we evaluated the CO<sub>2</sub> capture-desorption performance of 3-(dimethylamino)propylamine-6-propylene oxide (DMAPA-6PO), as a surface-active tertiary amine for cyclic CO<sub>2</sub> capture as bicarbonate. Results delineate a distinct CO<sub>2</sub> capture pathway utilizing DMAPA-6PO, which not only promotes bicarbonate generation, but also enhances CO<sub>2</sub> solubilization. This enhancement is attributed to the surface activity, based on <sup>13</sup>C nuclear magnetic resonance (NMR) and Fourier transform infrared spectroscopy (FTIR) analyses. Furthermore, DMAPA-6PO demonstrated a stable cyclic capacity, maintaining the CO<sub>2</sub> capture performance and bicarbonate concentration profiles over 900 min of testing cycles. We also examined the CO<sub>2</sub> capture capacity regeneration efficiency and desorption heat requirement in comparison with those of common commercial solvents. DMAPA-6PO showed a capture capacity regeneration efficiency that was 30% higher than that of monoethanolamine (MEA). Additionally, it exhibited a superior desorption rate, resulting in a substantial reduction of 88% in the heat duty requirements compared to MEA. The results demonstrate that DMAPA-6PO is a promising surface-active tertiary amine for capturing CO<sub>2</sub>, offering significant advantages in both the CO<sub>2</sub>-capture-as-bicarbonate pathway and traditional amine-based thermal desorption process.



## 1. INTRODUCTION

As the world is struggling with the pressing issue of increasing carbon emissions and their profound impact on climate change, exploring innovative solutions toward achieving carbon neutrality and a sustainable future has reached an unprecedented level of importance. Long-term projections emphasize the necessity of large-scale implementation of carbon capture, utilization, and storage (CCUS) technologies to meet emission reduction goals. Amine-based post-combustion capture (PCC) is currently the most proven and widely adopted technology for large-scale CCUS applications.<sup>1–3</sup>

The development of a techno-economically optimal CO<sub>2</sub> capture solvent is a key challenge in CCUS. An optimal CO<sub>2</sub> capture solvent possesses specific characteristics, including a high CO<sub>2</sub> cyclic capacity, efficient mass transfer, rapid CO<sub>2</sub> desorption, efficient regeneration, and stable long-term recyclability under operating conditions.<sup>4,5</sup> The cyclic capacity and regeneration efficiency are critical parameters that influence the amount of solution and thus the size of the equipment, such as the absorber columns required in practical applications. These factors subsequently contribute to the overall capital cost of CO<sub>2</sub> capture plants.<sup>6–9</sup> Notably, efficient desorption is crucial as it significantly impacts the regeneration energy requirements, which is the major component of the total energy consumption in PCC, accounting for 60–80% of the energy requirements. It also ensures that the absorbed CO<sub>2</sub>

is released from the solvent at lower energy costs, facilitating the readiness of the solvent for successive capture cycles.<sup>10–12</sup> Furthermore, the generation of degradation compounds during CO<sub>2</sub> capture reactions affects the CO<sub>2</sub> absorption capacity. This effect can also lead to increased corrosion, foaming, fouling, and environmental risks by generating potentially harmful substances such as volatile compounds and nitrosamines.

In this regard, extensive testing at Niederaussem pilot plant has provided insights into the degradation of monoethanolamine (MEA) over prolonged periods of thermal desorption. The specific MEA consumption per ton of captured CO<sub>2</sub> ranged from 0.21 to 3.65 kg MEA per ton of CO<sub>2</sub>. This variation was attributed to solvent degradation under different long-term thermal stress conditions without solvent reclaiming. However, implementing mitigation methods such as solvent reclamation and pretreatment significantly increases the overall operating cost.<sup>13,14</sup> Therefore, assessing the amine solvent regeneration and ensuring the stability of the CO<sub>2</sub> capture

Received: March 13, 2024

Revised: June 8, 2024

Accepted: June 26, 2024

Published: July 11, 2024



pathway are crucial for the performance and cost-effectiveness of amine-based CO<sub>2</sub> capture.

Researchers have extensively investigated various amine formulations and capture mechanisms to develop stable solvents with superior CO<sub>2</sub> capture and regeneration efficiencies. Absorption is the primary mechanism in amine-based systems, where CO<sub>2</sub> chemically reacts with the solvent to form compounds such as carbamates and bicarbonates. Additionally, in some technologies, adsorption plays a significant role, wherein CO<sub>2</sub> molecules physically adhere to the surfaces of solids or liquids without undergoing chemical reactions.<sup>15,16</sup> Research on amine-based chemical absorption has expanded to the reaction pathways and kinetics of amine interactions with CO<sub>2</sub>. Primary and secondary amines exhibit rapid CO<sub>2</sub> reaction rates, forming stable carbamates and releasing significant absorption heat, which necessitates a significant amount of energy for regeneration. In contrast, tertiary amines react to form unstable carbamates, which promote bicarbonate formation by hydrolysis, resulting in less energy consumption but a slower CO<sub>2</sub> absorption rate.<sup>17–20</sup> Consequently, many researchers have explored tertiary diamines such as DMAPA, DMBTA (*N,N*-dimethyl-1,4-butanediamine), blended amine formulations, like MEA/MDEA (methyl diethanolamine), and different configurations with the addition of mesoporous catalyst loadings.<sup>18,21–24</sup> Some researchers have also considered alternative pathways, such as integrating amine-based CO<sub>2</sub> capture with electrochemical conversion.<sup>25–27</sup> Despite these efforts, challenges still persist regarding solvent regeneration and degradation.

A promising alternative to the conventional “CO<sub>2</sub>-catch-and-release” process is to capture CO<sub>2</sub> as bicarbonate and use the resulting bicarbonate in a less energy-intensive CCUS pathway. The high thermal energy required to remove CO<sub>2</sub> and regenerate amine has always been a drawback of this process. In contrast, tertiary amines react to promote bicarbonate formation by hydrolysis, resulting in lower energy consumption. Therefore, capturing CO<sub>2</sub> using an efficient tertiary amine can provide a less energy-intensive carbon capture pathway. This approach can be coupled with the electrochemical conversion of bicarbonate into chemicals such as formate/formic acid, carbon monoxide, and others,<sup>28,29</sup> thereby establishing an integrated CO<sub>2</sub>-as-bicarbonate value chain for CCUS technologies. This pathway offers an effective, stable, and energy-efficient approach for storing and delivering CO<sub>2</sub>-bearing products into utilization units in aqueous carbon capture technologies. Notably, substituting CO<sub>2</sub> gas feed streams with captured bicarbonate improves the mass transfer rates of CO<sub>2</sub> gas in aqueous carbon capture technologies by a factor of 100, achieved through a higher carbon concentration in saturated solutions (3.3 M for saturated KHCO<sub>3</sub> compared to 0.033 M for saturated CO<sub>2</sub>).<sup>30</sup> Additionally, the electrochemical reduction of bicarbonate into formic acid consumes approximately 50% less energy than reducing CO<sub>2</sub> gas.<sup>29,31,32</sup> Hence, the potential of an amine solvent capable of delivering high CO<sub>2</sub> cyclic capacity, significant bicarbonate production, and superior regeneration capability holds great promise to advance this bicarbonate pathway.

In a prior publication by our research group focused on this bicarbonate pathway, we studied enhanced *in situ* bicarbonate generation during CO<sub>2</sub> capture by introducing surface activity into a tertiary amine.<sup>33</sup> We specifically employed 3-(dimethylamino)propylamine (DMAPA), a diamine containing both tertiary and primary amino groups. To create built-in

surface-active amines, we chemically introduced propylene groups (PO) at various levels to the primary amino group, resulting in DMAPA-*x*PO, where *x* represents 4, 6, 8, or 12, indicating the PO levels. The surface-active DMAPA-*x*PO solutions were shown by <sup>13</sup>C NMR analysis to produce only bicarbonate during the CO<sub>2</sub> capture process. The introduction of surface activity notably improved CO<sub>2</sub> capture, consequently enhancing the bicarbonate generation capacity of the amine solution. Optimal performance was observed with a PO level of 6 in DMAPA-6PO, with higher PO levels exhibiting a decline in CO<sub>2</sub> capture performance due to steric effects from higher carbon chains. This optimized level in DMAPA-6PO led to an enhancement of 54% in bicarbonate generation in comparison to DMAPA.<sup>33</sup> However, further critical assessment is necessary to substantiate the viability of DMAPA-6PO for large-scale deployment within the proposed integrated pathway for CO<sub>2</sub> capture as bicarbonate. These gaps primarily entail the comprehensive evaluation of the effect of the surface activity on the recyclability, chemical stability, regeneration efficiency, cyclic capture reaction pathway, and energy consumption of the amine solvent in comparison to commonly used commercial solvents.

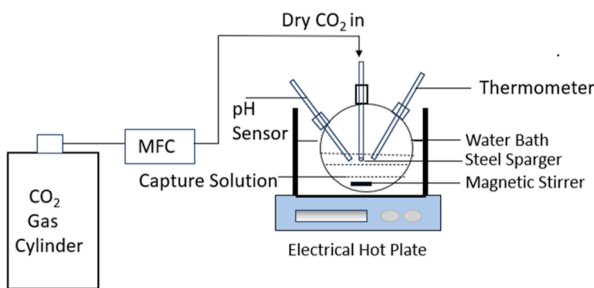
CO<sub>2</sub> desorption by thermal stripping is a suitable procedure to evaluate the mentioned critical parameters. By conducting these experiments, we will provide valuable information regarding this new class of tertiary amines utilized in the CO<sub>2</sub>-as-bicarbonate pathway useful to minimize the gap toward large-scale application. However, it is worth mentioning that releasing CO<sub>2</sub> from bicarbonate product is not originally envisioned within this proposed bicarbonate pathway. In contrast, separating bicarbonate to be used directly as a feedstock to produce chemicals while deprotonating the amine with an alkaline reaction for reutilization purposes is the target strategy to reduce the overall energy consumption of the amine-based CO<sub>2</sub> capture technology. The latter separation and regeneration operations are out of the scope of this publication. Therefore, this study focuses on investigating the cyclic performance, recyclability, and chemical stability of DMAPA-6PO in extended cycles of CO<sub>2</sub> capture as bicarbonate and thermal desorption. We present the reaction pathway of the solvent, showing the impact of the PO group derived from surface activity on enhanced CO<sub>2</sub> solubilization and bicarbonate generation and their subsequent desorption. Additionally, we assess the effect of temperature on the cyclic capacity and bicarbonate generation. Lastly, we evaluate the critical parameters of DMAPA-6PO, such as the CO<sub>2</sub> loading and bicarbonate cyclic capacity, regeneration efficiency, desorption rate, and heat duty, in comparison to MEA and DMAPA. We conducted these assessments using a laboratory-scale CO<sub>2</sub> capture and desorption setup, a modified Chittick titration setup, and spectroscopic analysis.

## 2. EXPERIMENTAL SECTION

**2.1. Chemicals.** Analytical grade chemical supplies of DMAPA-6PO (Harcros Chemicals, > 98.0%), DMAPA (Harcros Chemicals, > 98.0%), MEA (J. T. Baker, > 98.5%), and EDTA-4Na (Sigma-Aldrich, > 99.0%) were used without additional purification steps. 3N hydrochloric acid (HCl) from Thermo Fisher Scientific and methyl orange indicator powder from Aqua Solutions were used for titration. High-purity carbon dioxide (99.9% CO<sub>2</sub>) and nitrogen (99.998% N<sub>2</sub>) gases were sourced from Linde Gas & Equipment, Inc. Deionized water with a resistivity value of 18.2 MΩ/cm was used for all the experiments performed in this research.

**2.2. CO<sub>2</sub> Capture and Desorption Experiments.** The CO<sub>2</sub> capture setup is depicted in **Scheme 1**, as previously described in our

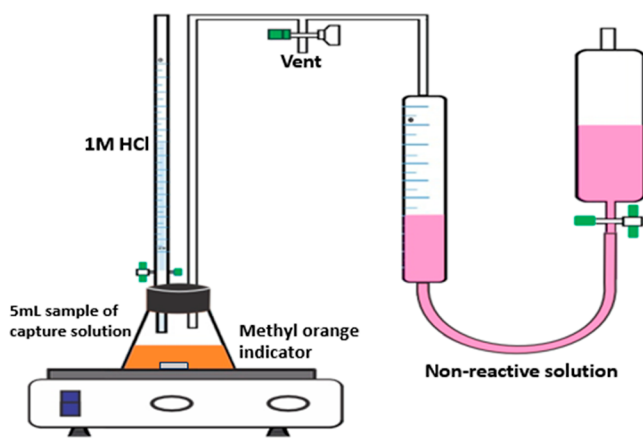
### Scheme 1. CO<sub>2</sub> Capture Experimental Setup



previous publication.<sup>33</sup> The reactor (250 mL four-necked flask) contained 200 mL of 0.1 mol/L of the desired aqueous amine solution. The solution was consistently stirred using a spherical magnetic stirring bar at a rotation speed of 250 rpm throughout the experiments. The reaction was carried out at ambient temperature and pressure conditions. CO<sub>2</sub> was continuously supplied at a precise flow rate of 90 mL/min regulated by a gas mass flow controller (FMA5508A-ST-CO<sub>2</sub> model by OMEGA Engineering Inc.). The CO<sub>2</sub> gas was bubbled through the solution via a stainless-steel sparger with a mean pore size of 2–10 μm at a pressure of 137 kPa for a duration of 75 min. The pH of the solution was continuously monitored during the tests using a Fisher Scientific Accumet AE150 pH meter. After the CO<sub>2</sub> capture process, a 6 mL aliquot of the reaction mixture was extracted for subsequent analyses, including CO<sub>2</sub> loading determination by titration and chemical characterization using spectroscopic measurements.

The titration for determining the CO<sub>2</sub> loading was performed using the Chittick apparatus illustrated in **Scheme 2**.<sup>34,35</sup> The Chittick setup

### Scheme 2. Chittick Titration Setup



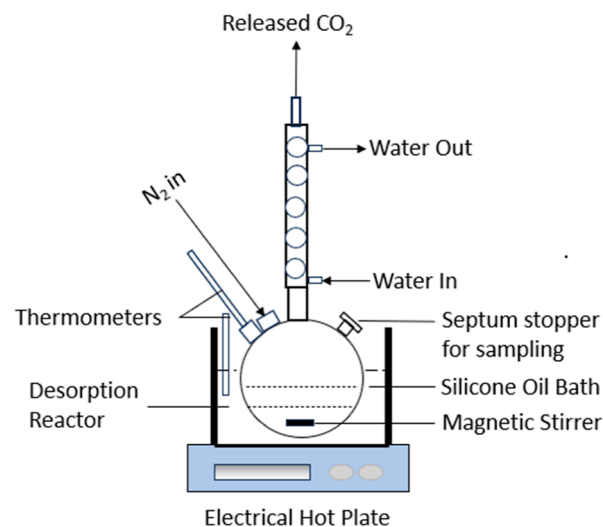
was modified from our previous setup to allow for air venting after each run of experiment to expedite the equilibration process. To calculate the CO<sub>2</sub> loading at ambient temperature and pressure, 5 mL of the extracted aliquot was transferred to an Erlenmeyer flask containing 50 mL of DI water. Two drops of 0.01 wt % methyl orange indicator were added to the flask, which was then tightly fitted to the buret with a cork to prevent the escape of gas from the system. Subsequently, the captured solution was treated with 1 mol/L of HCl while closely monitoring the color change from yellow to orange to ensure the complete release of CO<sub>2</sub> gas from the sample. The CO<sub>2</sub> loading, which quantifies the amount of CO<sub>2</sub> absorbed, was determined by measuring the volume of the nonreactive solution mixture (H<sub>2</sub>SO<sub>4</sub>, NaHCO<sub>3</sub>, and NaCl) displaced by the CO<sub>2</sub> gas that evolved from the titration reaction using the following formula<sup>35,36</sup>

$$\alpha_{\text{CO}_2} = \frac{\text{mol of CO}_2}{\text{mol of amine}} = \frac{\frac{P(V_{\text{gas}} - V_{\text{HCl}})}{RT}}{C_0 V_0} \quad (1)$$

where  $\alpha_{\text{CO}_2}$  is defined as the CO<sub>2</sub> loading, which is the mol of CO<sub>2</sub> captured per mole of the amine, R is the gas constant (8.314 L kPa/mol·K), P is the atmospheric pressure (kPa), T is the temperature (K), C<sub>0</sub> is the concentration of the sample (mol/L), V<sub>0</sub> is the volume of the sample (mL), V<sub>gas</sub> refers to the volume of released CO<sub>2</sub> determined by measuring the volume of the nonreactive solution displaced (mL), and V<sub>HCl</sub> is the volume of the acid consumed during the titration (mL). All titration results exhibited a high level of reproducibility, with deviations of no more than 2%.

After completing the CO<sub>2</sub> capture process, the CO<sub>2</sub> capture solution was subjected to thermal treatment for CO<sub>2</sub> desorption. The setup employed is shown in **Scheme 3**, where the four-neck flask

### Scheme 3. CO<sub>2</sub> Desorption Experimental Setup



containing the CO<sub>2</sub>-rich amine solution was fitted with a condenser to prevent the evaporation of water and the amine solution during the desorption. Nitrogen gas (N<sub>2</sub>) was introduced into the headspace of the reactor to maintain a deoxygenated system. The heating was carried out in a silicone oil bath (Grainger, 99.9%) at atmospheric pressure and constant temperature of 80 °C, using an electric hot plate coupled with continuous magnetic stirring (Thermo Fisher, ± 1.8 °C). The temperature of the amine solution was monitored throughout the heating process using a thermometer (Durac, ± 1.5 °C). The solution was initially heated for 15 min to attain thermal equilibrium with oil. Subsequently, samples of 6 mL each were collected at 10 min intervals to determine the CO<sub>2</sub> loading and perform instrumental analysis. The desorption process was stopped when a constant CO<sub>2</sub> loading was obtained.

In our capture-desorption cyclic assessment, we used both cyclic capacity and capture capacity regeneration efficiency as crucial parameters of evaluation.<sup>37</sup> The cyclic capacity is determined at equilibrium and is defined as the difference between the maximum CO<sub>2</sub> loading after CO<sub>2</sub> capture (also defined as the CO<sub>2</sub> capture capacity) and the minimum CO<sub>2</sub> loading after desorption (also defined as the desorption capacity).<sup>38,39</sup> On the other hand, the capture capacity regeneration efficiency is determined by the ratio of the cyclic capacity to the CO<sub>2</sub> capture capacity. An additional parameter calculated from the CO<sub>2</sub> desorption reaction is the desorption rate (mmol CO<sub>2</sub>/min·L). For this purpose, a linear correlation within the initial 10 min of desorption between the CO<sub>2</sub> loading and time was established. This evaluation is essential since industrial processes do not always reach equilibrium due to practical limitations.<sup>6</sup>

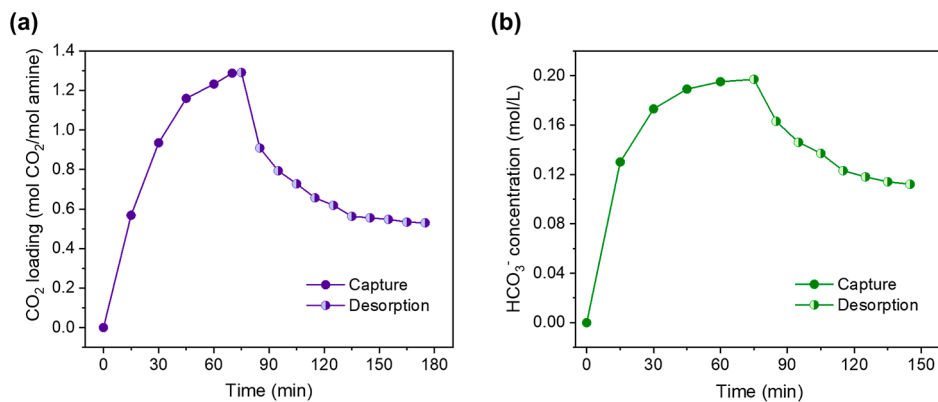


**Figure 1.** (a) CO<sub>2</sub> capture and desorption profile of 0.1 mol/L DMAPA-6PO; the CO<sub>2</sub> loading values are within a standard deviation of  $\pm 0.02$  mol CO<sub>2</sub>/mol amine. (b) Bicarbonate product concentration during CO<sub>2</sub> capture and desorption using 0.1 mol/L DMAPA-6PO. The bicarbonate concentration values were within a standard deviation of  $\pm 0.01$  mol CO<sub>2</sub>/mol amine. In both (a,b), CO<sub>2</sub> capture was performed at room temperature and 90 mL CO<sub>2</sub>/min, while CO<sub>2</sub> desorption was at a constant temperature of 80 °C.

The heat duty, measuring the heat needed for solvent regeneration after CO<sub>2</sub> capture, is a critical parameter that accounts for nearly 70% of overall expenses, thus serving as a pivotal metric for capture solution comparison and process optimization.<sup>40</sup> The heat duty (kJ/mmol CO<sub>2</sub>) was calculated from the desorption rate and heat input using Fourier's law of heat transfer and is given as follows<sup>41</sup>

$$\text{heat duty} = \frac{\text{heat input}}{\text{desorption rate}} = \frac{\frac{kA(\Delta T)}{d}}{I_d} \quad (2)$$

where  $k$  is defined as the thermal conductivity of the reactor (1.2 J/s·m·K),  $A$  is the area of the heat transfer (0.00318 m<sup>2</sup>),  $\Delta T$  is the difference in temperature between inside and outside the reactor (K),  $d$  is the thickness of the reactor (0.25 cm), and  $I_d$  is the calculated desorption rate (mmol CO<sub>2</sub>/min·L).

**2.3. Instrumental Analysis.** NMR spectroscopy was used for quantifying bicarbonate, elucidating reaction pathways/species, and assessing the stability of the solvent throughout the reaction. 0.5 mL of the capture solution was treated with 100  $\mu$ L of deuterium oxide (Thermo Scientific, NMR 99.8 atom % D) to establish a system lock. Tetramethylammonium chloride (Acros Organics, 98+%) was used as a reference peak to calibrate the other secondary peaks. The tubes were tightly sealed to prevent material exchange with the surrounding environment. The analytical procedures were conducted using a Bruker Avance Neo 400 NMR machine at ambient temperature with a relaxation delay time of 2 and 1024 scans. The bicarbonate concentration was quantified by a calibration curve using <sup>13</sup>C NMR for pure sodium bicarbonate (ThermoFisher Scientific, > 95%) using previously established methods.<sup>33</sup> The NMR results were processed using the MestNova software for baseline and phase correction before interpreting the results.

Similarly, FTIR was employed for qualitative analysis of the chemical changes and to check the stability and possible degradation of the solvent during the CO<sub>2</sub> capture and desorption processes. The spectral data were acquired using a Bruker Invenio-R instrument. Transmittance (%) measurements were recorded at 10 min intervals during the desorption process, maintaining a signal-to-noise ratio of 100 between the sample and the background. The forward and reverse velocities were consistently set at 50 kHz. Each spectrum was recorded with the acquisition of 256 scans for both the sample and background, employing a resolution of 4 and a signal gain of 1. The bandwidth number of the instrument covered a range from 400 to 4000 cm<sup>-1</sup>.

### 3. RESULTS

#### 3.1. CO<sub>2</sub> Capture and Desorption Performance of DMAPA-6PO.

Figure 1a presents the CO<sub>2</sub> capture and desorption performance of 0.1 mol/L DMAPA-6PO solution.

The CO<sub>2</sub> capture process was carried out at ambient temperature. In this condition, the surface-active amine demonstrated a rapid CO<sub>2</sub> capture process, attaining slightly over 40% of its total CO<sub>2</sub> capture capacity 15 min after the CO<sub>2</sub> capture reaction started. In addition, a maximum CO<sub>2</sub> loading capacity of 1.29 mol CO<sub>2</sub>/mol amine was achieved after 75 min of reaction, similar to our previous report.<sup>33</sup> Based on a preliminary extended experiment shown in Figure S1, the surface-active amine became fully saturated with CO<sub>2</sub> after 70 min of CO<sub>2</sub> capture. Beyond this point, the amine solution maintained a constant loading capacity. Therefore, 75 min was selected as the final CO<sub>2</sub> capture time for this and the subsequent experiments.

After the CO<sub>2</sub> capture process, the CO<sub>2</sub> desorption was performed with a constant 80 °C heat treatment until a steady CO<sub>2</sub> loading capacity value of 0.53 mol CO<sub>2</sub>/mol amine is attained. Notably, this resulted in an initial capture capacity regeneration of 59%, associated with a CO<sub>2</sub> cyclic capacity of 0.76 mol CO<sub>2</sub>/mol amine, for the DMAPA-6PO solution. The CO<sub>2</sub> desorption profile revealed that approximately 30% of the total CO<sub>2</sub> desorption process occurred within the initial 10 min of heating, as the CO<sub>2</sub> loading decreased from 1.29 to 0.91 mol CO<sub>2</sub>/mol amine, thus indicating a rapid desorption kinetics.

Since the bicarbonate (HCO<sub>3</sub><sup>-</sup>) is the main product derived from the CO<sub>2</sub> capture reaction using DMAPA-6PO, the bicarbonate concentration profile was also monitored during the capture and desorption of CO<sub>2</sub>. This profile is presented in Figure 1b. As the CO<sub>2</sub> capture reaction started, the bicarbonate concentration rapidly increased, until it reached a maximum of 0.20 mol/L, in concordance with the CO<sub>2</sub> capture performance presented in Figure 1a. Then, during the CO<sub>2</sub> desorption process, the bicarbonate concentration decreased to a constant value of 0.11 mol/L after 70 min of the heat treatment. Thus, the bicarbonate cyclic capacity (as defined in Section 2.2) was 0.09 mol/L. Then, the estimated capacity of DMAPA-6PO to regenerate bicarbonate from capturing CO<sub>2</sub> in a consecutive cycle was calculated to be 44%. Table 1 summarizes all evaluated parameters derived from the CO<sub>2</sub> capture and desorption assessments using 0.1 mol/L DMAPA-6PO solution.

Another important observation is the decrement of the bicarbonate concentration during the CO<sub>2</sub> desorption process. Table 1 indicates that the bicarbonate concentration decreased

**Table 1. Evaluated Parameters from the CO<sub>2</sub> Capture and Desorption Experiments Using 0.1 mol/L DMAPA-6PO Solution<sup>c</sup>**

parameter	capture capacity	desorption capacity	cyclic capacity	capture capacity regeneration (%)
CO <sub>2</sub> loading <sup>a</sup> (mol CO <sub>2</sub> /mol amine)	1.29	0.53	0.76	59
HCO <sub>3</sub> <sup>-</sup> concentration <sup>b</sup> (mol/L)	0.20	0.11	0.09	44

<sup>a</sup>CO<sub>2</sub> loading STD:  $\pm 0.02$  mol CO<sub>2</sub>/mol amine. <sup>b</sup>HCO<sub>3</sub><sup>-</sup> concentration STD:  $\pm 0.01$  mol/L. <sup>c</sup>Note: CO<sub>2</sub> capture was carried out at room temperature and 90 mL CO<sub>2</sub>/min, whereas CO<sub>2</sub> was desorbed at a constant temperature of 80 °C.

by approximately 44% during the heating process, associated with its decomposition to release CO<sub>2</sub> gas. It has been demonstrated that pure ammonium bicarbonate solution is thermally decomposed within the 60–95 °C range for liberation of CO<sub>2</sub>,<sup>42</sup> which covers our experimental conditions at 80 °C. Therefore, if all the decrements in bicarbonate resulted in CO<sub>2</sub> gas, the 44% value was too low to account for the 59% obtained from the CO<sub>2</sub> loading parameter. This discrepancy suggests that there is a contribution from solubilized CO<sub>2</sub>, which is not converted into bicarbonate during the capture process.

We carried out a blank experiment, in which 0.2 mol/L NaHCO<sub>3</sub> solution was prepared to simulate the highest bicarbonate concentration produced after CO<sub>2</sub> saturation from the capture process. The solution was then titrated using the same process, and the CO<sub>2</sub> loading was determined. This blank bicarbonate solution corresponded to an equivalent CO<sub>2</sub> loading amount (eCO<sub>2</sub> loading) of 1.25 mol CO<sub>2</sub>/mol amine. This value is slightly lower than the CO<sub>2</sub> loading obtained from the titration of the CO<sub>2</sub> saturated amine (1.29 mol CO<sub>2</sub>/mol amine), indicating a contribution of 0.04 mol CO<sub>2</sub>/mol amine from the dissolved CO<sub>2</sub> at the end of the capture process. Based on this blank experiment, a correlation factor between the obtained eCO<sub>2</sub> loading and the NaHCO<sub>3</sub> concentration values was calculated to be 6.28 mol CO<sub>2</sub>/L/mol amine·mol HCO<sub>3</sub><sup>-</sup>. This correlation factor was then used to calculate the subsequent eCO<sub>2</sub> loadings derived from the measured HCO<sub>3</sub><sup>-</sup> concentration via <sup>13</sup>C NMR throughout the desorption process. The resulting values are presented in Figure 2.

As expected, the eCO<sub>2</sub> loadings from the bicarbonate decomposition during the desorption process were lower than the CO<sub>2</sub> loading values obtained for the desorbed amine solution. The difference between the two values increased as the desorption process began with the heat treatment, reaching a maximum difference of 0.15 mol CO<sub>2</sub>/mol amine when the desorption process was completed. This difference can be attributed to the amount of CO<sub>2</sub> dissolved in the capture solution that was not converted into bicarbonate. Therefore, this amount, representing 11% of the total CO<sub>2</sub> loading capacity after the heating, could not be quantified from the bicarbonate peaks obtained in the NMR analysis. These results clearly demonstrate the ability of the surface-active amine to not only capture CO<sub>2</sub> as bicarbonate, but also to enhance the solubility of CO<sub>2</sub> in the aqueous media.

With the aim of assessing the stability and recyclability of the DMAPA-6PO solution, consecutive CO<sub>2</sub> capture-desorption

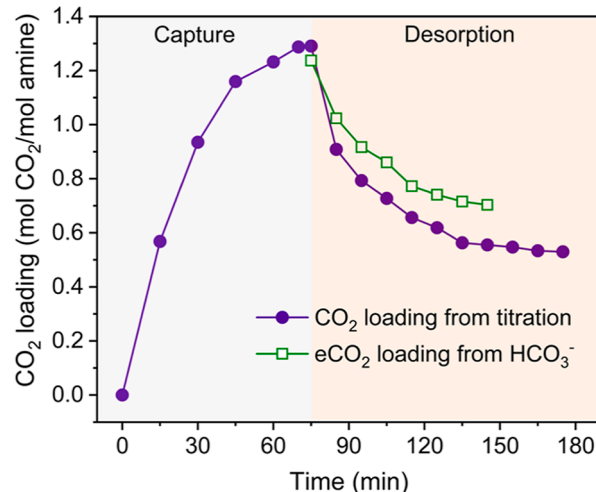


**Figure 2.** Comparison between the experimental CO<sub>2</sub> loading from titration and equivalent CO<sub>2</sub> loading (eCO<sub>2</sub> loading) from bicarbonate concentration obtained from <sup>13</sup>C NMR analysis. CO<sub>2</sub> capture was carried out at room temperature and 90 mL CO<sub>2</sub>/min, while CO<sub>2</sub> desorption was at a constant temperature of 80 °C. All the CO<sub>2</sub> loading and eCO<sub>2</sub> loading values are within a standard deviation of  $\pm 0.02$  mol CO<sub>2</sub>/mol amine and  $\pm 0.06$  mol CO<sub>2</sub>/mol amine, respectively.

cycles were carried out as presented in Figure 3. A 6-cycle performance was explored in terms of both the CO<sub>2</sub> loading

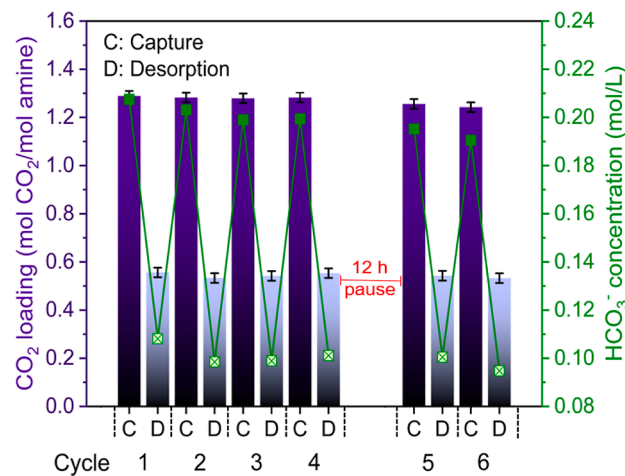


**Figure 3.** CO<sub>2</sub> loading and bicarbonate concentration profiles over six consecutive CO<sub>2</sub> capture-desorption cycles performed by 0.1 mol/L DMAPA-6PO. CO<sub>2</sub> capture was carried out at room temperature and 90 mL CO<sub>2</sub>/min for 75 min, while CO<sub>2</sub> desorption was at a constant temperature of 80 °C for 75 min (total time of 150 min/cycle).

and the bicarbonate concentration analysis. As can be observed (on the left Y-axis in Figure 3), the surface-active amine maintained consistent maximum and minimum CO<sub>2</sub> loading capacities following the capture and desorption processes throughout all the tested cycles. As for the CO<sub>2</sub> capture, the average CO<sub>2</sub> loading was determined to be 1.27 mol CO<sub>2</sub>/mol amine. Similarly, for the desorption process, the average CO<sub>2</sub> loading stood at 0.54 mol CO<sub>2</sub>/mol amine. However, a slight decrement of 4% in initial capture capacity was observed at the end of the sixth cycle, which could be attributed to the DMAPA-6PO degradation over the consecutive heat treatments.<sup>14,43</sup> In terms of the CO<sub>2</sub> cyclic capacity, a slight

decrease from 0.75–0.71 mol CO<sub>2</sub>/mol amine was observed when the last cycle finished. Despite this drop, the CO<sub>2</sub> capture capacity regeneration remained within the range of 57–58%, thus validating the stability and recyclability of the surface-active amine solution. All the values obtained for the CO<sub>2</sub> loading capacity are listed in Table 2.

**Table 2. Evaluated Parameters from the CO<sub>2</sub> Loading Determination during the Consecutive CO<sub>2</sub> Capture-desorption Cycles Using 0.1 mol/L DMAPA-6PO<sup>b</sup>**

cycle	capture capacity <sup>a</sup> (mol CO <sub>2</sub> /mol amine)	desorption capacity <sup>a</sup> (mol CO <sub>2</sub> /mol amine)	cyclic capacity <sup>a</sup> (mol CO <sub>2</sub> /mol amine)	capture capacity regeneration (%)
1	1.29	0.56	0.73	57
2	1.28	0.53	0.75	58
3	1.28	0.54	0.74	58
4	1.28	0.55	0.73	57
5	1.26	0.54	0.71	57
6	1.24	0.53	0.71	57

<sup>a</sup>CO<sub>2</sub> loading STD:  $\pm 0.02$  mol CO<sub>2</sub>/mol amine. <sup>b</sup>Note: CO<sub>2</sub> capture was carried out at room temperature and 90 mL CO<sub>2</sub>/min for 75 min, while CO<sub>2</sub> desorption at a constant temperature of 80 °C for 75 min (total time of 150 min/cycle).

As performed for the CO<sub>2</sub> loading capacity, the bicarbonate concentration was also monitored over the consecutive CO<sub>2</sub> capture-desorption cycles (right Y-axis in Figure 3). The average bicarbonate concentration produced from the capture process was 0.20 mol/L, while the average concentration after the desorption process was 0.10 mol/L. In detail, the maximum bicarbonate concentration generated in the first cycle was 0.21 mol/L, which decreased to 0.19 mol/L at the end of the sixth cycle, representing a drop of 8% after consecutive 900 min of testing. Notably, the bicarbonate cyclic capacity and the bicarbonate capture capacity regeneration remained consistent over the consecutive test cycles, with the range of 0.10–0.09 mol/L and 48–50%, respectively. All the values are presented in Table 3. This bicarbonate analysis revealed that the ability of DMAPA-6PO to regenerate bicarbonate from capturing CO<sub>2</sub> in consecutive capture-desorption cycles is well maintained despite the decrement in the maximum and minimum bicarbonate concentration values per cycle. This consistency demonstrates its suitability as an effective solvent for capturing CO<sub>2</sub> as bicarbonate.

**Table 3. Evaluated Parameters from the Bicarbonate Concentration during the Consecutive CO<sub>2</sub> Capture-Desorption Cycles Using 0.1 mol/L DMAPA-6PO<sup>b</sup>**

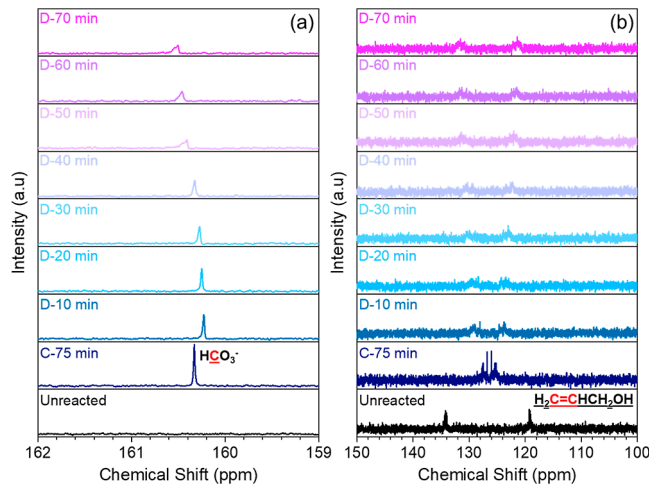
cycle	capture capacity <sup>a</sup> (mol/L)	desorption capacity <sup>a</sup> (mol/L)	cyclic capacity <sup>a</sup> (mol/L)	capture capacity regeneration (%)
1	0.21	0.11	0.10	48
2	0.20	0.10	0.10	52
3	0.20	0.10	0.10	50
4	0.20	0.10	0.10	49
5	0.20	0.10	0.09	49
6	0.19	0.09	0.10	50

<sup>a</sup>HCO<sub>3</sub><sup>-</sup> concentration STD:  $\pm 0.01$  mol/L. <sup>b</sup>Note: CO<sub>2</sub> capture was carried out at room temperature and 90 mL CO<sub>2</sub>/min for 75 min, while CO<sub>2</sub> desorption was at a constant temperature of 80 °C for 75 min (total time of 150 min/cycle).

Lastly, a potential degradation effect in the consecutive CO<sub>2</sub> capture-desorption cycles was studied by introducing a 12 h pause break between the fourth and fifth cycle to assess the stability and resilience of the surface-active amine solution under conditions simulating operational interruptions such as venting, that typically occur in practical settings.<sup>44</sup> This pause allowed us to isolate the possibility of degradation effects over time without continuous or additional CO<sub>2</sub> streams. During this pause, the surface-active amine solution was allowed to rest inside the closed reactor without any nitrogen flow at the end of the fourth cycle. When the fifth cycle was resumed, it was observed that this break showed no significant impact on the bicarbonate concentrations or CO<sub>2</sub> loading capacities of DMAPA-6PO. The measured values remained consistent with the existing trend. This is reflected by a marginal decline in performance, corresponding to a drop of 2% in CO<sub>2</sub> cyclic capacity and a drop of 4% in the bicarbonate cyclic capacity between the mentioned cycles, as already observed in the overall trend. This minimal decline in the surface-active amine performance provides strong evidence of its stability under practical stress conditions.

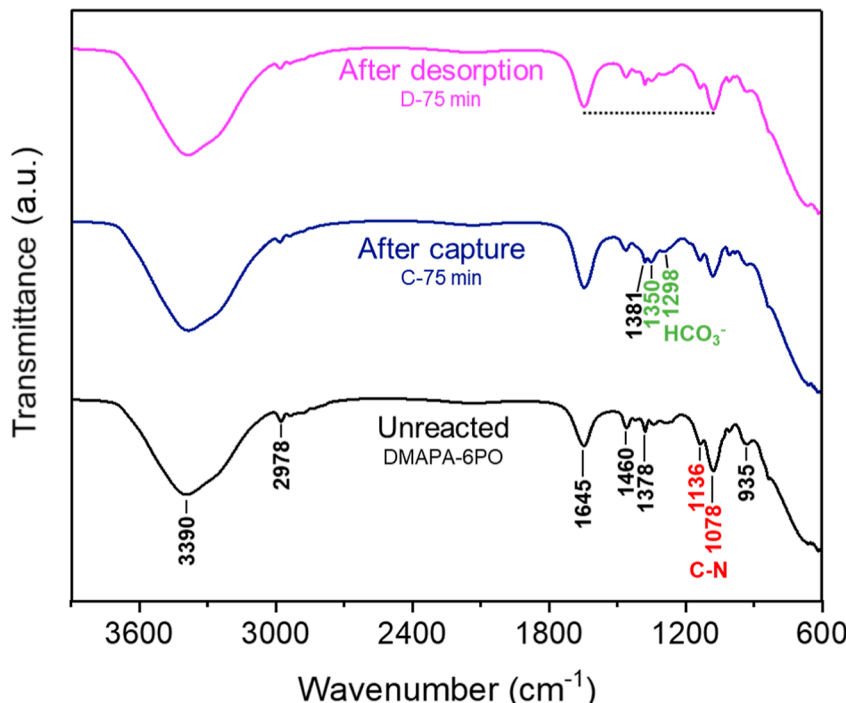
**3.2. Chemical Reactions during CO<sub>2</sub> Capture and Desorption.** To fully harness the full potential of DMAPA-6PO as a CO<sub>2</sub> capture solvent, it is crucial to have a comprehensive understanding of the intricate mechanisms and species involved in the reactions. This includes the evolution of the bicarbonate, the effect of the surface activity, protonation changes occurring at the amino groups, as well as any intermediate observations. These factors collectively influence the efficacy and stability of the cyclic reaction pathway of the solvent. A detailed explanation of this process is provided in the subsequent sections through NMR and FTIR analyses.

Figure 4 shows the obtained spectra from <sup>13</sup>C NMR analysis. DMAPA-6PO samples were taken before the reaction with



**Figure 4.** <sup>13</sup>C NMR spectra of 0.1 mol/L DMAPA-6PO solution before CO<sub>2</sub> capture (unreacted), after CO<sub>2</sub> capture (C-75 min), and after CO<sub>2</sub> desorption at 80 °C (D-10 to D-70 min).

CO<sub>2</sub>, after equilibrium, and during desorption at 80 °C at 10 min intervals. The spectra in Figure 4a specifically show the evolution of the bicarbonate generated during the CO<sub>2</sub> capture and desorption reactions. At the initial stage, no bicarbonate signal was observed in the unreacted sample. After 75 min of CO<sub>2</sub> capture reaction (C-75 min), the equilibrium state was reached, and a new peak emerged at 160.4 ppm represented



**Figure 5.** FTIR spectra of 0.1 mol/L DMAPA-6PO solution before CO<sub>2</sub> capture (unreacted), after CO<sub>2</sub> capture (C-75 min), and after CO<sub>2</sub> desorption at 80 °C (D-75 min).

bicarbonate.<sup>45</sup> At this point, the bicarbonate species reached a maximum concentration of 0.21 mol/L. No additional peaks related to carbonate or carbamate were detected after CO<sub>2</sub> capture, as shown in the full spectrum of Figure S2.

During the desorption reaction, the bicarbonate peak underwent a distinct intensity reduction. Initially, it sharply decreased from its maximum concentration attained during CO<sub>2</sub> capture to a substantially smaller peak observed after 10 min (D-10 min), indicating rapid decomposition kinetics in comparison to other periods. This decrease then continued steadily until it reached an end point after 70 min of desorption (D-70 min), with a final concentration of 0.11 mol/L. In this stage, only a minimal reduction in the peak intensity was observed, indicating the presence of residual undecomposed bicarbonate. This finding aligns with the observed 50% capacity regeneration of bicarbonate, as shown in Table 3.

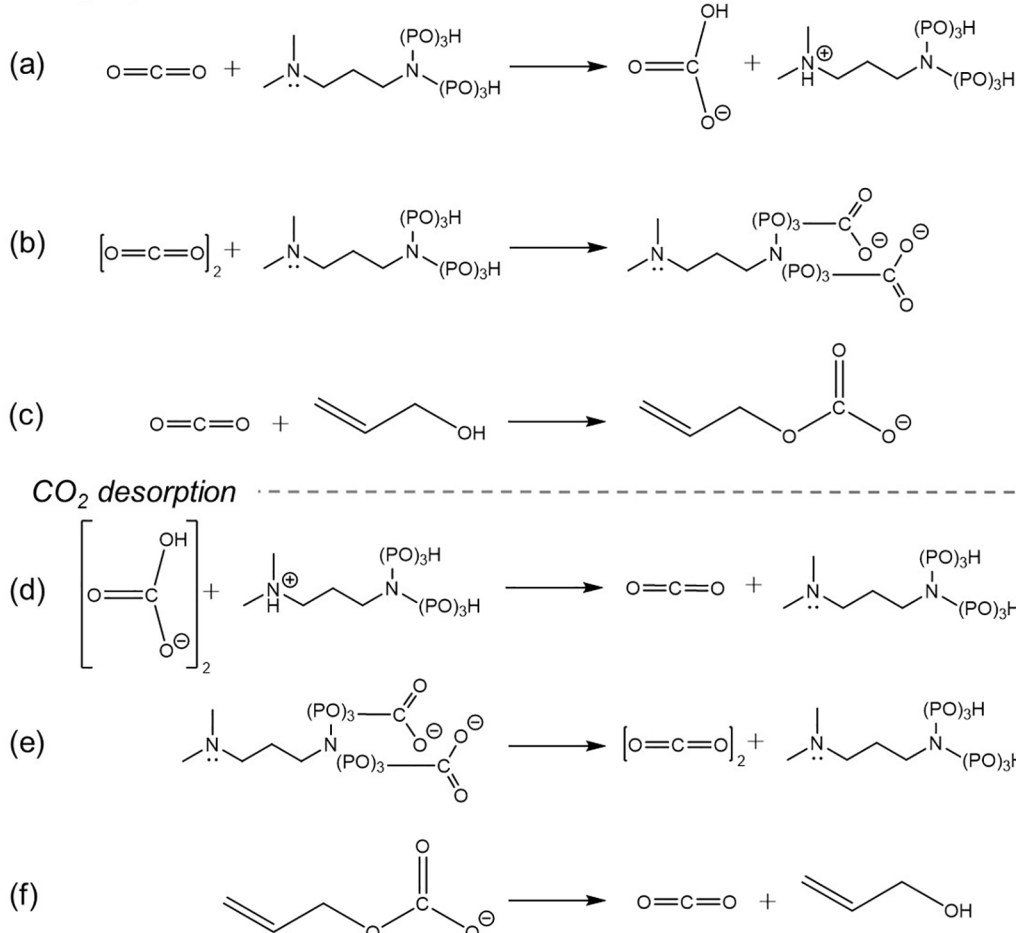
Interestingly, two peaks at 119.2 and 134.1 ppm were observed during the <sup>13</sup>C NMR analysis for the unreacted DMAPA-6PO sample. These peaks are associated with the C=C bond found in the allyl alcohol (C<sub>3</sub>H<sub>5</sub>OH), a common R-OH byproduct produced during the propoxylation of DMAPA.<sup>46</sup> Although its presence could be considered as a trace due to the low intensity of its C-C double bond signals, this allyl alcohol marginally contributed to the CO<sub>2</sub> capture and desorption mechanism, as depicted in Figure 4b.

After the CO<sub>2</sub> capture reaction (C-75 min), the two signals of the allylic carbons are closely shifted to approximately 126 ppm. This shift could be attributed to the interaction between the electron-rich hydroxyl group from the allyl alcohol and the electron-deficient carbon in the CO<sub>2</sub> molecule, thus forming a protonated base with C<sub>3</sub>H<sub>5</sub>O-C=OO<sup>-</sup> structure.<sup>47</sup> Consequently, the strong resonance effect of the new environment composed of the -O-C=OO<sup>-</sup> group, shifted the sp<sup>2</sup> carbon resonance from the vinyl group to lower frequencies.<sup>48</sup> During the desorption process, these peak signals gradually returned to

their initial frequencies over the heating time upon reaching the end point (D-70 min), as observed for bicarbonate. This shift could be attributed to the breakdown of the -O-C=OO<sup>-</sup> group, leading to the gradual release of the captured CO<sub>2</sub>.

Similar trends are observed in the pH variations presented in Figure S3 of Supporting Information. Following CO<sub>2</sub> capture, the pH value gradually declined from its initial level of 11.9, reaching a minimum of 6.9 after 70 min, which is in concordance with the bicarbonate generation results shown in Figure 1b. Throughout the desorption phase, a gradual reversion to the initial basicity was observed, which was evidenced by a rise in pH from the minimum of 6.9 to approximately 9.0. This event was associated with a decrease in bicarbonate concentration due to thermal decomposition, as presented in Figures 1b and 4a. However, it is noteworthy that pH did not fully recover to its initial value of 11.9, indicating an incomplete regeneration in line with prior discussions. All these chemical changes represent the fundamental basis for a recyclable CO<sub>2</sub> capture process.

FTIR was used to corroborate the reaction species and chemical alterations during both capture and desorption processes. Figure 5 depicts the spectra of DMAPA-6PO for the unreacted, after CO<sub>2</sub> capture (C-75 min), and after desorption (D-75 min) samples for comparison. Before the exposure to CO<sub>2</sub>, the unreacted DMAPA-6PO displayed characteristic C-N stretching modes at 1078 and 1136 cm<sup>-1</sup>, related to symmetric and asymmetric stretch, respectively.<sup>49</sup> Notably, the C=C wagging vibration from allyl alcohol was identified at 935 cm<sup>-1</sup>,<sup>50</sup> corroborating the previous observations from <sup>13</sup>C NMR analysis. Additional contributions attributed to C-H bending modes were present at 1378 and 1460 cm<sup>-1</sup>,<sup>49</sup> whereas the sharp signal at 2978 cm<sup>-1</sup> is related to the C-H stretching mode.<sup>51</sup> The two bands present at 1645

$\text{CO}_2$  capture

**Figure 6.** Proposed mechanism of  $\text{CO}_2$  capture and desorption reactions using DMAPA-6PO solution.

and  $3390\text{ cm}^{-1}$  are associated with the O–H bending and O–H stretching modes of the water molecule, respectively.<sup>51</sup>

Upon analysis after  $\text{CO}_2$  capture, some distinct changes were observed in the spectrum of the C-75 min sample. New vibration bands emerged at  $1298$  and  $1350\text{ cm}^{-1}$ , corresponding to the C–OH bending and symmetric C=OO<sup>−</sup> stretching associated with bicarbonate formation,<sup>49</sup> respectively. The additional signal located at  $1381\text{ cm}^{-1}$  could be assigned to the antisymmetric stretching of the  $\text{CO}_3^{2-}$  ion,<sup>52</sup> as stated in the literature. Nevertheless, after completing the  $\text{CO}_2$  capture reaction, only bicarbonate was observed in the  $^{13}\text{C}$  NMR results. Moreover, under the final pH value of  $6.9$ , the carbonate species concentration has been reported to be low (<0.001%).<sup>53</sup> Thus, this double degenerate stretching signal suggests the presence of the –O–C=OO<sup>−</sup> group formed by the  $\text{CO}_2$  interaction with –OH groups in the DMAPA-6PO solution, as previously discussed in Figure 4b. This scenario involves not only the hydroxyl groups from the allyl alcohol byproduct but also the incorporated surface activity by the 6PO groups, contributing to an enhanced  $\text{CO}_2$  solubilization that is not represented as bicarbonate formation, as discussed in Section 3.1. The formation of this –O–C=OO<sup>−</sup> group can be referred to as an intrinsic and intermediate trapping mechanism derived from the built-in surface activity that increases the dissolved  $\text{CO}_2$  amount in the aqueous media and contributes to the total amount of  $\text{CO}_2$  released but not as bicarbonate product from the amino group, as evidenced by

the difference between the  $\text{CO}_2$  loading and the e $\text{CO}_2$  loading from pure bicarbonate solution presented in Figure 2.

Another important observation after  $\text{CO}_2$  capture (C-75 min) is related to DMAPA-6PO protonation. This chemical alteration associated with the NH<sup>+</sup> band is typically seen around  $1650\text{ cm}^{-1}$ ,<sup>49</sup> but it overlaps with the water molecule vibrating mode at  $1645\text{ cm}^{-1}$ . Despite this, an evident transmittance increment of this band with respect to the unreacted sample was observed, along with a decrement of the C–N bands at  $1078$  and  $1136\text{ cm}^{-1}$ . As DMAPA-6PO protonates, the concentration of free C–N bonds is expected to be reduced, showing a smaller band intensity while the NH<sup>+</sup> concentration increases. This effect was reversed at the end of the desorption process (D-70 min), where both signals exhibited similar band intensities (C–N slightly higher), in concordance with the  $\text{CO}_2$  capture capacity regeneration results listed in Table 2.

To corroborate this observation, the ratio between the C–N signal (denoted as A) and NH<sup>+</sup> signal containing the OH contribution (denoted as B) was calculated and is presented in Figure S4. For the unreacted sample, the initial A/B ratio is  $1.39$ . This value corroborates the high availability of the active sites for  $\text{CO}_2$  capture. After completing the capture reaction, the A/B ratio decreased to  $0.45$ , indicating the decrease in the free C–N active sites and the increase in NH<sup>+</sup> concentration. Finally, this A/B ratio was calculated to be  $0.82$  at the end of  $\text{CO}_2$  desorption, demonstrating the regeneration capacity of

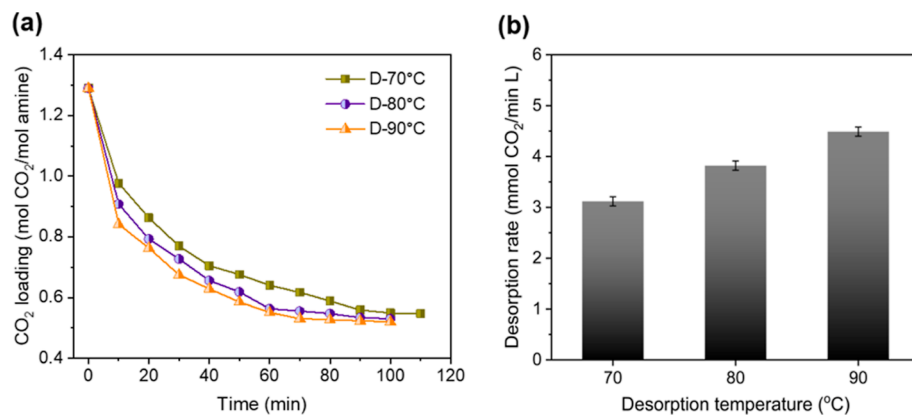


**Figure 7.** (a) Desorption profile of 0.1 mol/L DMAPA-6PO at 70, 80, and 90 °C. The CO<sub>2</sub> loading values are within a standard deviation of  $\pm 0.02$  mol CO<sub>2</sub>/mol amine; (b) calculated desorption rate within the initial 10 min of reaction at given temperatures. CO<sub>2</sub> capture was carried out at room temperature and 90 mL CO<sub>2</sub>/min for 75 min, up to a CO<sub>2</sub> loading of 1.29 mol CO<sub>2</sub>/mol amine.

the C–N active sites by amine deprotonation. Although this partial regeneration of the free nitrogen sites of DMAPA-6PO impacts the total amount of the captured CO<sub>2</sub> in the subsequent reaction (reflected in the cyclic capacity variation), the capture capacity regeneration is maintained around 57% over consecutive tests, as presented in Figure 3 and Table 2. The latter result indicates the strong capacity of DMAPA-6PO to keep capturing and releasing the same CO<sub>2</sub> ratio on constant assessments despite the final loading amount determined by titration.

A simplified speciation relating CO<sub>2</sub> capture and desorption reactions utilizing DMAPA-6PO solution is illustrated in Figure 6. During the capture process, the nitrogen sites of the DMAPA-6PO serve as a proton acceptor reacting with CO<sub>2</sub> in the form of carbonic acid, generating both bicarbonate and protonated amine species (Figure 6a), as reported in our previous publication.<sup>33</sup> Simultaneously, the –OH groups from the propoxylated amine (Figure 6b) and the allyl alcohol (Figure 6c) derived from the incorporated surface activity attack the electron-deficient carbon within the CO<sub>2</sub> molecule, resulting in the formation of an intermediate base characterized by the –O–C=OO<sup>–</sup> group, which improves the solubilization of CO<sub>2</sub> in the aqueous media until an equilibrium state is reached. In the desorption process, the generated bicarbonate is partially decomposed to CO<sub>2</sub> while the deprotonation of DMAPA-6PO takes place, as shown in Figure 6d. In addition, the intermediate base from the propoxylated amine (Figure 6e) and allyl alcohol (Figure 6f) is broken down by the thermal treatment releasing the captured CO<sub>2</sub>.

The built-in surface activity was demonstrated to be an important component during the CO<sub>2</sub> capture and desorption steps. As mentioned before, it contributes to the enhanced dissolution of CO<sub>2</sub> as an additional trapping mechanism, which is then reflected in the higher CO<sub>2</sub> desorption amount. To corroborate this effect, we conducted a comparative analysis between DMAPA-6PO and ethylenediaminetetraacetic acid tetrasodium salt (EDTA-4Na), another industrially used solvent with two tertiary amino groups but without surface activity. The results demonstrated a 30% higher CO<sub>2</sub> loading amount and 46% higher capture capacity regeneration using the amine with a built-in surface activity, as shown in Figure S5. The superior performance of DMAPA-6PO highlights the suitable characteristics for an enhanced CO<sub>2</sub> capture capacity.

### 3.3. Desorption Performance at Different Temperatures.

Optimizing the temperature for the desorption process while generating bicarbonate is crucial for balancing reaction kinetics and energy consumption. Therefore, we examined the effects of different temperatures on the desorption performance of DMAPA-6PO, in terms of desorption rate and bicarbonate concentration. We compared our previous CO<sub>2</sub> desorption reaction carried out at 80 °C (presented in Section 3.1) with new experiments conducted at 70 and 90 °C. This selection was deliberately focused on temperatures that were sufficiently high for desorption but remained below the boiling point of the solvent to prevent excessive water evaporation and unnecessary energy loss.

Figure 7a depicts the CO<sub>2</sub> loading profile of DMAPA-6PO during desorption for all the temperatures. The time required to reach an equilibrium state was extended as the desorption temperature decreased. For instance, the equilibration time at 70 °C was prolonged up to 90 min, which is 10 and 20 min longer than the time at 80 and 90 °C, respectively. The average CO<sub>2</sub> loading at this equilibrium state was around 0.53 mol CO<sub>2</sub>/mol amine in all cases. However, a slightly better desorption performance was observed at 90 °C with the lowest CO<sub>2</sub> loading of 0.52 mol CO<sub>2</sub>/mol amine, compared with 0.53 and 0.54 mol CO<sub>2</sub>/mol amine for 80 and 70 °C, respectively.

Another observation is the rapid CO<sub>2</sub> desorption step observed in the initial 10 min for all temperatures. From the starting point, the CO<sub>2</sub> loading decreased considerably to the total amount desorbed. For the process carried out at 70 °C, a decrease of 32% was calculated within 10 min of reaction, while 42 and 53% were obtained at 80 and 90 °C, respectively. Despite identifying this initial period as a determining step in the desorption mechanism, it is clear that increasing the desorption temperature accelerated the reaction kinetics. Figure 7b shows the impact of temperature on the calculated initial desorption rate within the initial 10 min of reaction. The straight-line correlation is shown in Figure S6. An increase in temperature from 70 to 90 °C increased the desorption rate from 3.12 mmol CO<sub>2</sub>/min·L to 4.49 mmol CO<sub>2</sub>/min·L, indicating a clear dependence of the desorption kinetics on the desorption temperature.

Likewise, the bicarbonate concentrations after 75 min of heating at 70, 80, and 90 °C are depicted in Figure 8. As can be seen, the bicarbonate concentration reached the lowest value of 0.11 mol/L when the desorption was carried out at 80 and

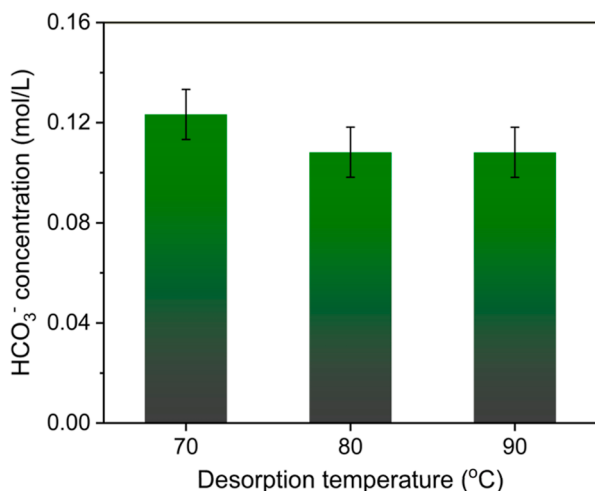


**Figure 8.** Bicarbonate concentration after 75 min of desorption at 70, 80, and 90 °C utilizing 0.1 mol/L DMAPA-6PO.

90 °C. However, at the lowest temperature of 70 °C, the bicarbonate concentration was slightly higher (0.12 mol), which was 12% higher than that obtained at higher temperatures. This result is in concordance with that observed in Figure 7 and confirms a slower bicarbonate decomposition at lower temperatures.

Additionally, the CO<sub>2</sub> cyclic capacity at 75 min varied accordingly, as shown in Figure S7. At low temperature, the cyclic capacity was reduced due to the small amount of CO<sub>2</sub> released. The CO<sub>2</sub> cyclic capacity at 70 °C was determined to be 0.69 mol CO<sub>2</sub>/mol amine, which increased around 7–8% at 80 °C. Interestingly, this cyclic capacity further increased by only 2% with the desorption reaction at 90 °C. Therefore, 80 °C was found to be the optimal temperature to perform the CO<sub>2</sub> desorption reaction from the DMAPA-6PO solution. The subsequent desorption experiments in Section 3.4 were conducted at a controlled temperature of 80 °C.

**3.4. Comparison with Different Capture Solutions.** To investigate the overall CO<sub>2</sub> capture-desorption performance of DMAPA-6PO relative to established commercial amine capture solutions, we conducted a comparative analysis using 3-(dimethylamino)propylamine (DMAPA) and monoethanolamine (MEA) as benchmarks. DMAPA was chosen as the base amine compound for the synthesis of DMAPA-6PO, while

MEA was selected due to its widespread usage and well-documented characteristics within CO<sub>2</sub> capture applications.<sup>38</sup>

Figure 9a compares the CO<sub>2</sub> desorption profiles of the three capture solvents. The CO<sub>2</sub> capture reaction was carried out as described previously. The desorption reaction was performed at 80 °C until a constant CO<sub>2</sub> loading capacity was reached. As can be seen, DMAPA-6PO and DMAPA exhibited rapid desorption reactions compared to MEA. Moreover, both diamines reached a constant CO<sub>2</sub> loading amount after 70 min of heating, which was considerably shorter than the 100 min required for MEA. This observation suggests slower desorption kinetics for MEA, resulting in an extended stripping time compared to DMAPA-6PO and DMAPA. In this regard, the desorption rate from the straight portion of the curve was calculated and is illustrated in Figure 9b. All linear fittings are presented in Figure S8. For DMAPA-6PO, the calculated desorption rate was 3.77 mmol CO<sub>2</sub>/min L, significantly higher than that determined for DMAPA (0.97 mmol CO<sub>2</sub>/min L) and MEA (0.45 mmol CO<sub>2</sub>/min L). In terms of kinetics, it is clear that DMAPA-6PO outperforms the commercial solutions used.

To obtain more insightful information about the differences in the CO<sub>2</sub> release processes of these three capture solvents, the heat duty was calculated based on their desorption rates (Figure 9b). As expected, the lowest energy value was obtained for DMAPA-6PO (1.09 kJ/mmol CO<sub>2</sub>), followed by DMAPA (4.37 kJ/mmol CO<sub>2</sub>) and MEA (9.16 kJ/mmol CO<sub>2</sub>). Consistently, the order in heat duty was opposite to that in the desorption rate; that is, the surface-active tertiary amine demonstrated outstanding desorption capabilities for the regeneration and release of the captured CO<sub>2</sub>. In particular, DMAPA-6PO required 75% less heat than DMAPA and 88% less heat than MEA.

The faster desorption and lower heat duty of DMAPA-6PO than those of DMAPA and MEA are attributed not only to the effects of its built-in surface activity, as previously described in Sections 3.1 and 3.2, but also to the differences in their chemical characteristics in the CO<sub>2</sub> capture reaction. The surface activity in DMAPA-6PO leads to enhanced solubilization of CO<sub>2</sub> in aqueous amine solution and the generation of bicarbonate instead of the carbamates formed in MEA and DMAPA.<sup>33</sup> From an energy perspective, it requires less heat to release CO<sub>2</sub> from bicarbonate decomposition, which has a lower heat of formation compared to breaking the more stable C–N bond of carbamate, leading to higher energy

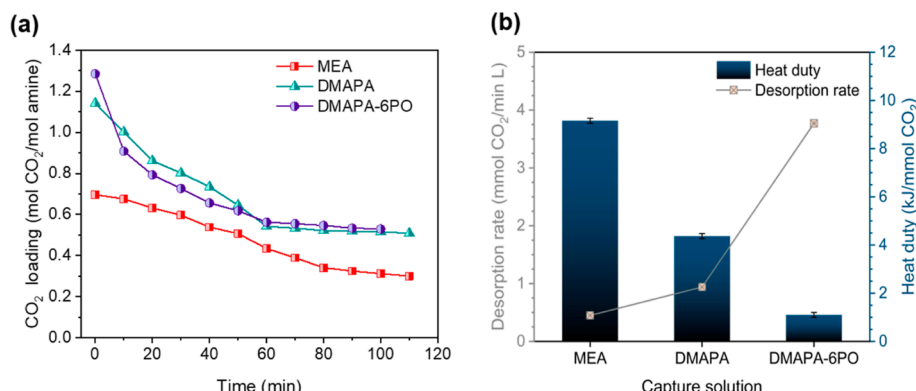


**Figure 9.** (a) CO<sub>2</sub> desorption profiles of 0.1 mol/L DMAPA-6PO, DMAPA, and MEA carried out at 80 °C for 100 min; (b) relationship between the calculated desorption rate and heat duty at 80 °C.

consumption for  $\text{CO}_2$  liberation.<sup>20</sup> This distinction is particularly pronounced in MEA, which primarily generates carbamate, resulting in higher heat of reaction and vaporization, consequently requiring a larger heat duty.<sup>54</sup>

Since the three amines possess differences in the type and number of the amino groups, it is crucial to integrate these intrinsic properties of each capture solution in a standardized comparison. Therefore, Figure 10 depicts the normalized  $\text{CO}_2$

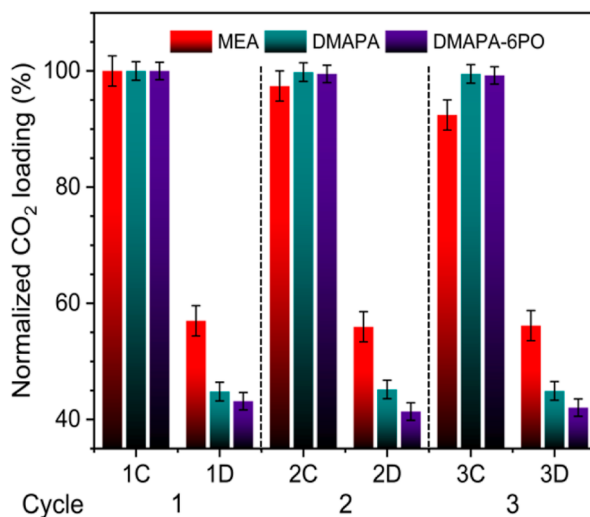


**Figure 10.** Normalized  $\text{CO}_2$  loading capacity over three consecutive  $\text{CO}_2$  capture-desorption cycles performed by 0.1 mol/L DMAPA-6PO, DMAPA, and MEA.  $\text{CO}_2$  capture was carried out at room temperature and 90 mL  $\text{CO}_2$ /min for 75 min, while  $\text{CO}_2$  desorption was carried at a constant temperature of 80 °C for 75 min (total time of 150 min/cycle).

loading capacity for the three solvents across three cycles of  $\text{CO}_2$  capture and desorption, showcasing their overall capture-desorption performance. It can be seen that DMAPA-6PO and DMAPA maintained a relatively constant  $\text{CO}_2$  cyclic capacity, with minimum variations during the three consecutive cycles. DMAPA-6PO showed an average capture capacity regeneration of 57%, which is greater than that of DMAPA, 55%. This higher performance is related to the low  $\text{CO}_2$  loading capacity at the end of the desorption process in each cycle, for which the amount of  $\text{CO}_2$  desorbed was 7% greater than that by DMAPA. This difference can be attributed to the higher bicarbonate generation of DMAPA-6PO in comparison to DMAPA, as confirmed in our previous work,<sup>33</sup> and to the solubilized  $\text{CO}_2$  observed in Figure 2, which contributes to the total amount of  $\text{CO}_2$  released.

**Table 4.** Cyclic Capacities and the Regeneration Efficiencies of 0.1 mol/L MEA, DMAPA, and DMAPA-6PO Solutions over Three Cycles of  $\text{CO}_2$  Capture and Desorption<sup>b</sup>

cycle	MEA		DMAPA		DMAPA-6PO	
	cyclic capacity <sup>a</sup> (mol $\text{CO}_2$ /mol amine)	capture capacity regeneration (%)	cyclic capacity <sup>a</sup> (mol $\text{CO}_2$ /mol amine)	capture capacity regeneration (%)	cyclic capacity <sup>a</sup> (mol $\text{CO}_2$ /mol amine)	capture capacity regeneration (%)
1	0.29	43	0.63	55	0.73	57
2	0.28	42	0.63	55	0.74	57
3	0.25	39	0.63	55	0.74	57

<sup>a</sup> $\text{CO}_2$  loading STD:  $\pm 0.02$  mol  $\text{CO}_2$ /mol amine. <sup>b</sup>Note:  $\text{CO}_2$  capture was carried out at room temperature and 90 mL  $\text{CO}_2$ /min for 75 min, while  $\text{CO}_2$  desorption at a constant temperature of 80 °C for 75 min (total time of 150 min/cycle).

In contrast, a decreasing performance was observed for the MEA case where its initial capture capacity regeneration, 43%, was reduced to 40% at the end of the third cycle. The capture capacity regeneration of DMAPA-6PO was 30% greater than that of MEA. For the capture process, the initial  $\text{CO}_2$  loading capacity was reduced by 3% at the second cycle and 5% at the third cycle. This result is associated with the reduction in  $\text{CO}_2$  loading capacity due to solvent degradation after the heating process of each cycle, aligning with previously reported findings.<sup>55</sup> Table 4 provides an overview of the cyclic capture capacities and regeneration efficiencies over the three cycles.

In terms of  $\text{CO}_2$  mass, a larger amount of  $\text{CO}_2$  was captured by DMAPA-6PO than by MEA because the additional amino group led to a  $\text{CO}_2$  loading capacity of 1.29 mol  $\text{CO}_2$ /mol amine, as shown in Table S1. However, during desorption, DMAPA-6PO also released a larger amount of  $\text{CO}_2$  than MEA, as evidenced by its higher  $\text{CO}_2$  cyclic capacity. In other words, DMAPA-6PO is capturing and releasing a larger amount of  $\text{CO}_2$  with less heat than MEA, the most utilized amine-based capture solution. An overall perspective is summarized in Figure 11, which shows the high performance of DMAPA-6PO considering its  $\text{CO}_2$  cyclic capacity and low heat requirement.

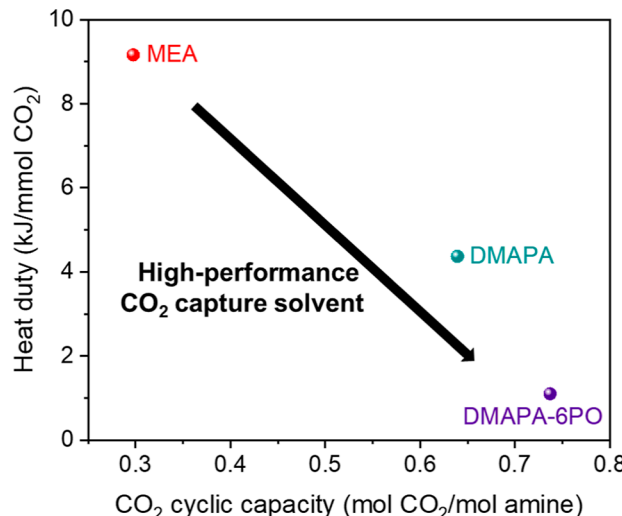


**Figure 11.** Summarized comparison between DMAPA-6PO, DMAPA, and MEA on their  $\text{CO}_2$  cyclic capacity and heat duty performance during  $\text{CO}_2$  capture-desorption reaction.

This evaluation demonstrates the potential advantages of developing a surface-active amine as a  $\text{CO}_2$  capture solvent over conventional amine-based capture solutions. These advantages are mainly based on the optimized reaction pathway during  $\text{CO}_2$  capture, which not only increases the

carbon content in the aqueous solution through enhanced bicarbonate concentration and solubilized CO<sub>2</sub>, but also improves CO<sub>2</sub> release performance in the conventional heat stripping process. Nevertheless, it is important to note that this study, conducted under controlled conditions, presents opportunities for future research to further optimize the performance of DMAPA-6PO as a CO<sub>2</sub> capture solvent. Further investigations could explore higher concentrations or industrial flue gas compositions with contaminants like NO<sub>x</sub> and SO<sub>x</sub>, which are known to affect and accelerate degradation.<sup>14,56</sup> Additionally, assessing the stability and efficiency of the amine solvent under elevated pressure conditions, as well as the effect of continuous cyclic use on the active nitrogen sites, is pertinent for industrial upscale applications.

## 4. CONCLUSIONS

We investigated the CO<sub>2</sub> capture-desorption performance of DMAPA-6PO as a promising solvent for capturing CO<sub>2</sub> as bicarbonate. The experimental results confirmed the remarkable cyclic capacity and stability of DMAPA-6PO during consecutive capture–desorption cycles, exhibiting only a reduction of 4% in capture capacity observed after 900 min of testing. This performance was also evidenced in the bicarbonate generation capacity, with a drop of 8% at the end of the evaluation. The CO<sub>2</sub> capture capacity regeneration of DMAPA-6PO was 30% greater than that of MEA under low desorption temperature (80 °C). In addition, DMAPA-6PO demonstrated a notably high rate of desorption, resulting in a reduction of 88% in the required heat duty in comparison to MEA. This enhanced efficiency is attributed to the bicarbonate generation from CO<sub>2</sub> capture derived from the built-in surface activity of DMAPA-6PO, which improves the CO<sub>2</sub> solubilization in aqueous media and facilitates the CO<sub>2</sub> release process from the heating process. Based on these results, the development and utilization of surface-active amines are promising strategies when considering their application in the CO<sub>2</sub>-capture-as-bicarbonate pathway and the conventional stripping process for releasing captured CO<sub>2</sub>.

## ■ ASSOCIATED CONTENT

### SI Supporting Information

The Supporting Information is available free of charge at <https://pubs.acs.org/doi/10.1021/acs.energyfuels.4c01208>.

Extended CO<sub>2</sub> loading and pH profiles for DMAPA-6PO during CO<sub>2</sub> capture and desorption reactions, as well as the comparative analysis with EDTA-4Na and additional amine characterization results such as <sup>13</sup>C NMR and FTIR ([PDF](#))

## ■ AUTHOR INFORMATION

### Corresponding Author

Omar A. Carrasco-Jaim – The Center for Subsurface Energy and the Environment, The University of Texas at Austin, Austin, Texas 78712, United States;  [0000-0001-9850-217X](https://orcid.org/0000-0001-9850-217X); Email: [oacarrasco@utexas.edu](mailto:oacarrasco@utexas.edu)

### Authors

Abdulmuiz A. Adekom – The Center for Subsurface Energy and the Environment, The University of Texas at Austin, Austin, Texas 78712, United States

Upali P. Weerasooriya – The Center for Subsurface Energy and the Environment, The University of Texas at Austin, Austin, Texas 78712, United States

Ryosuke Okuno – The Center for Subsurface Energy and the Environment, The University of Texas at Austin, Austin, Texas 78712, United States

Complete contact information is available at:  
<https://pubs.acs.org/10.1021/acs.energyfuels.4c01208>

### Author Contributions

Abdulmuiz A. Adekom: Methodology, validation, formal analysis, investigation, data curation, writing—original draft, and visualization. Omar A. Carrasco-Jaim: Methodology, validation, formal analysis, investigation, data curation, writing—review and editing, and visualization. Upali P. Weerasooriya: Methodology, validation, formal analysis, and resources. Ryosuke Okuno: Conceptualization, methodology, validation, formal analysis, resources, writing—review and editing, supervision, project administration, and funding acquisition.

### Notes

The authors declare no competing financial interest.

## ■ ACKNOWLEDGMENTS

This research was performed as part of the Energi Simulation Industrial Affiliate Program on Carbon Utilization and Storage (ES CarbonUT) at the Center for Subsurface Energy and the Environment at The University of Texas at Austin. Ryosuke Okuno holds the Pioneer Corporation Faculty Fellowship in Petroleum Engineering at the University of Texas at Austin. Additionally, we appreciate the support provided by Harcros Chemicals Inc. in the preparation of the samples necessary for our study.

## ■ REFERENCES

- (1) Ling, H.; Gao, H.; Liang, Z. Comprehensive Solubility of N<sub>2</sub>O and Mass Transfer Studies on an Effective Reactive N,N-Dimethylethanolamine (DMEA) Solvent for Post-Combustion CO<sub>2</sub> Capture. *Chem. Eng. J.* **2019**, *355*, 369–379.
- (2) Wang, L.; Liu, S.; Wang, R.; Li, Q.; Zhang, S. Regulating Phase Separation Behavior of a DEEA–TETA Biphasic Solvent Using Sulfolane for Energy-Saving CO<sub>2</sub> Capture. *Environ. Sci. Technol.* **2019**, *53* (21), 12873–12881.
- (3) Xiao, M.; Liu, H.; Gao, H.; Olson, W.; Liang, Z. CO<sub>2</sub> Capture with Hybrid Absorbents of Low Viscosity Imidazolium-Based Ionic Liquids and Amine. *Appl. Energy* **2019**, *235*, 311–319.
- (4) Afkhamipour, M.; Mofarahi, M. Review on the Mass Transfer Performance of CO<sub>2</sub> Absorption by Amine-Based Solvents in Low- and High-Pressure Absorption Packed Columns. *RSC Adv.* **2017**, *7* (29), 17857–17872.
- (5) Shukla, C.; Mishra, P.; Dash, S. K. A Review of Process Intensified CO<sub>2</sub> Capture in RPB for Sustainability and Contribution to Industrial Net Zero. *Front. Energy Res.* **2023**, *11*, 1135188.
- (6) Luo, X.; Liu, S.; Gao, H.; Liao, H.; Tontiwachwuthikul, P.; Liang, Z. An Improved Fast Screening Method for Single and Blended Amine-Based Solvents for Post-Combustion CO<sub>2</sub> Capture. *Sep. Purif. Technol.* **2016**, *169*, 279–288.
- (7) Aronu, U. E.; Svendsen, H. F.; Hoff, K. A.; Juliusen, O. Solvent Selection for Carbon Dioxide Absorption. *Energy Procedia* **2009**, *1* (1), 1051–1057.
- (8) Aronu, U. E.; Svendsen, H. F.; Hoff, K. A. Investigation of Amine Amino Acid Salts for Carbon Dioxide Absorption. *Int. J. Greenhouse Gas Control* **2010**, *4* (5), 771–775.

- (9) Aronu, U. E.; Hoff, K. A.; Svendsen, H. F. CO<sub>2</sub> Capture Solvent Selection by Combined Absorption–Desorption Analysis. *Chem. Eng. Res. Des.* **2011**, *89* (8), 1197–1203.
- (10) Feng, B.; Du, M.; Dennis, T. J.; Anthony, K.; Perumal, M. J. Reduction of Energy Requirement of CO<sub>2</sub> Desorption by Adding Acid into CO<sub>2</sub>-Loaded Solvent. *Energy Fuels* **2010**, *24* (1), 213–219.
- (11) Zhang, S.; Du, M.; Shao, P.; Wang, L.; Ye, J.; Chen, J.; Chen, J. Carbonic Anhydrase Enzyme-MOFs Composite with a Superior Catalytic Performance to Promote CO<sub>2</sub> Absorption into Tertiary Amine Solution. *Environ. Sci. Technol.* **2018**, *52* (21), 12708–12716.
- (12) Zhang, X.; Zhang, X.; Liu, H.; Li, W.; Xiao, M.; Gao, H.; Liang, Z. Reduction of Energy Requirement of CO<sub>2</sub> Desorption from a Rich CO<sub>2</sub>-Loaded MEA Solution by Using Solid Acid Catalysts. *Appl. Energy* **2017**, *202*, 673–684.
- (13) Moser, P.; Wiechers, G.; Schmidt, S.; Garcia Moretz-Sohn Monteiro, J.; Charalambous, C.; Garcia, S.; Sanchez Fernandez, E. Results of the 18-Month Test with MEA at the Post-Combustion Capture Pilot Plant at Niederaussem – New Impetus to Solvent Management, Emissions and Dynamic Behaviour. *Int. J. Greenhouse Gas Control* **2020**, *95*, 102945.
- (14) Vefelstad, S. J.; Buvik, V.; Knuutila, H. K.; Grimstvedt, A.; Da Silva, E. F. Important Aspects Regarding the Chemical Stability of Aqueous Amine Solvents for CO<sub>2</sub> Capture. *Ind. Eng. Chem. Res.* **2022**, *61*, 15737.
- (15) Soo, X. Y. D.; Lee, J. J. C.; Wu, W.-Y.; Tao, L.; Wang, C.; Zhu, Q.; Bu, J. Advancements in CO<sub>2</sub> Capture by Absorption and Adsorption: A Comprehensive Review. *J. CO<sub>2</sub> Util.* **2024**, *81*, 102727.
- (16) Yu, C.-H.; Huang, C.-H.; Tan, C.-S. A Review of CO<sub>2</sub> Capture by Absorption and Adsorption. *Aerosol Air Qual. Res.* **2012**, *12* (5), 745–769.
- (17) Chowdhury, F. A.; Yamada, H.; Higashii, T.; Goto, K.; Onoda, M. CO<sub>2</sub> Capture by Tertiary Amine Absorbents: A Performance Comparison Study. *Ind. Eng. Chem. Res.* **2013**, *52* (24), 8323–8331.
- (18) Idem, R.; Wilson, M.; Tontiwachwuthikul, P.; Chakma, A.; Veawab, A.; Aroonwilas, A.; Gelowitz, D. Pilot Plant Studies of the CO<sub>2</sub> Capture Performance of Aqueous MEA and Mixed MEA/MDEA Solvents at the University of Regina CO<sub>2</sub> Capture Technology Development Plant and the Boundary Dam CO<sub>2</sub> Capture Demonstration Plant. *Ind. Eng. Chem. Res.* **2006**, *45* (8), 2414–2420.
- (19) Mimura, T.; Simayoshi, H.; Suda, T.; Iijima, M.; Mituoka, S. Development of Energy Saving Technology for Flue Gas Carbon Dioxide Recovery in Power Plant by Chemical Absorption Method and Steam System. *Energy Convers. Manage.* **1997**, *38*, S57–S62.
- (20) Monteiro, J. G. M.-S.; Pinto, D. D. D.; Zaidy, S. A. H.; Hartono, A.; Svendsen, H. F. VLE Data and Modelling of Aqueous N,N-Diethylethanolamine (DEEA) Solutions. *Int. J. Greenhouse Gas Control* **2013**, *19*, 432–440.
- (21) Bahamon, D.; Anlu, W.; Builes, S.; Khaleel, M.; Vega, L. F. Effect of Amine Functionalization of MOF Adsorbents for Enhanced CO<sub>2</sub> Capture and Separation: A Molecular Simulation Study. *Front. Chem.* **2021**, *8*, 574622.
- (22) Ko, Y. G.; Shin, S. S.; Choi, U. S. Primary, Secondary, and Tertiary Amines for CO<sub>2</sub> Capture: Designing for Mesoporous CO<sub>2</sub> Adsorbents. *J. Colloid Interface Sci.* **2011**, *361* (2), 594–602.
- (23) Li, S.; Kang, G. W.; Chen, J. Measurement and Thermodynamic Modeling for CO<sub>2</sub> Solubility in the N-(2-Hydroxyethyl)Piperazine + Water System. *Front. Energy Res.* **2021**, *9*, 785039.
- (24) Bairq, Z. A. S.; Gao, H.; Murshed, F. A. M.; Tontiwachwuthikul, P.; Liang, Z. Modified Heterogeneous Catalyst-Aided Regeneration of CO<sub>2</sub> Capture Amines: A Promising Perspective for a Drastic Reduction in Energy Consumption. *ACS Sustain. Chem. Eng.* **2020**, *8* (25), 9526–9536.
- (25) Li, M.; Yang, K.; Abdinejad, M.; Zhao, C.; Burdyny, T. Advancing Integrated CO<sub>2</sub> Electrochemical Conversion with Amine-Based CO<sub>2</sub> Capture: A Review. *Nanoscale* **2022**, *14* (33), 11892–11908.
- (26) Sullivan, I.; Goryachev, A.; Digdaya, I. A.; Li, X.; Atwater, H. A.; Vermaas, D. A.; Xiang, C. Coupling Electrochemical CO<sub>2</sub> Conversion with CO<sub>2</sub> Capture. *Nat. Catal.* **2021**, *4* (11), 952–958.
- (27) Sharifan, R.; Wagterveld, R. M.; Digdaya, I. A.; Xiang, C.; Vermaas, D. A. Electrochemical Carbon Dioxide Capture to Close the Carbon Cycle. *Energy Environ. Sci.* **2021**, *14* (2), 781–814.
- (28) Zhang, Z.; Xi, D.; Ren, Z.; Li, J. A Carbon-Efficient Bicarbonate Electrolyzer. *Cell Rep. Phys. Sci.* **2023**, *4* (11), 101662.
- (29) Li, T.; Lees, E. W.; Zhang, Z.; Berlinguette, C. P. Conversion of Bicarbonate to Formate in an Electrochemical Flow Reactor. *ACS Energy Lett.* **2020**, *5* (8), 2624–2630.
- (30) Li, T.; Lees, E. W.; Goldman, M.; Salvatore, D. A.; Weekes, D. M.; Berlinguette, C. P. Electrolytic Conversion of Bicarbonate into CO in a Flow Cell. *Joule* **2019**, *3* (6), 1487–1497.
- (31) Welch, A. J.; Dunn, E.; DuChene, J. S.; Atwater, H. A. Bicarbonate or Carbonate Processes for Coupling Carbon Dioxide Capture and Electrochemical Conversion. *ACS Energy Lett.* **2020**, *5* (3), 940–945.
- (32) Zhang, Z.; Lees, E. W.; Ren, S.; Huang, A.; Berlinguette, C. P. Electrolytic Conversion of Bicarbonate Solutions to CO at > 500 mA Cm<sup>-2</sup> and 2.2 V. *ChemRxiv* **2021**.
- (33) Carrasco-Jaim, O. A.; Xia, H.; Weerasooriya, U. P.; Okuno, R. CO<sub>2</sub> Capture as Bicarbonate Using DMAPA with Incorporation of Surface Activity. *Fuel* **2023**, *348*, 128554.
- (34) Huang, J.; Fisher, P. R.; Argo, W. R. A Gasometric Procedure to Measure Residual Lime in Container Substrates. *HortScience* **2007**, *42* (7), 1685–1689.
- (35) Norouzbahari, S.; Shahhosseini, S.; Ghaemi, A. Chemical Absorption of CO<sub>2</sub> into an Aqueous Piperazine (PZ) Solution: Development and Validation of a Rigorous Dynamic Rate-Based Model. *RSC Adv.* **2016**, *6* (46), 40017–40032.
- (36) Pichetwanit, P.; Kungsanan, S.; Supap, T. Effects of Surfactant Type and Structure on Properties of Amines for Carbon Dioxide Capture. *Colloids Surf., A* **2021**, *622*, 126602.
- (37) Bishnoi, S.; Rochelle, G. T. Absorption of Carbon Dioxide into Aqueous Piperazine: Reaction Kinetics, Mass Transfer and Solubility. *Chem. Eng. Sci.* **2000**, *55* (22), 5531–5543.
- (38) Kumar, S.; Mondal, M. K. Selection of Efficient Absorbent for CO<sub>2</sub> Capture from Gases Containing Low CO<sub>2</sub>. *Korean J. Chem. Eng.* **2020**, *37* (2), 231–239.
- (39) Zhang, R.; Yang, Q.; Liang, Z.; Puxty, G.; Mulder, R. J.; Cosgriff, J. E.; Yu, H.; Yang, X.; Xue, Y. Toward Efficient CO<sub>2</sub> Capture Solvent Design by Analyzing the Effect of Chain Lengths and Amino Types to the Absorption Capacity, Bicarbonate/Carbamate, and Cyclic Capacity. *Energy Fuels* **2017**, *31* (10), 11099–11108.
- (40) Saravanakumar; Kumar, S.; Krishna, A. Advances in CO<sub>2</sub> Capture Using Absorption and Adsorption Technology: A Review. *J. Emerg. Technol. Innov. Res.* **2021**, *8* (11), c733.
- (41) Wai, S. K.; Nwaoha, C.; Saiwan, C.; Idem, R.; Supap, T. Absorption Heat, Solubility, Absorption and Desorption Rates, Cyclic Capacity, Heat Duty, and Absorption Kinetic Modeling of AMP–DETA Blend for Post–Combustion CO<sub>2</sub> Capture. *Sep. Purif. Technol.* **2018**, *194*, 89–95.
- (42) Qing, Z.; Yincheng, G.; Zhenqi, N.; Wenyi, L. Investigation on Carbon Dioxide Regeneration from Ammonium Bicarbonate Solution in a Packed Reactor. In *2010 International Conference on Digital Manufacturing & Automation*; IEEE: Changsha, 2010; pp 870–873..
- (43) Sun, C.; Dutta, P. K. Infrared Spectroscopic Study of Reaction of Carbon Dioxide with Aqueous Monoethanolamine Solutions. *Ind. Eng. Chem. Res.* **2016**, *55* (22), 6276–6283.
- (44) Hamdy, L. B.; Goel, C.; Rudd, J. A.; Barron, A. R.; Andreoli, E. The Application of Amine-Based Materials for Carbon Capture and Utilisation: An Overarching View. *Mater. Adv.* **2021**, *2* (18), 5843–5880.
- (45) Zhang, R.; Yang, Q.; Yu, B.; Yu, H.; Liang, Z. Toward to Efficient CO<sub>2</sub> Capture Solvent Design by Analyzing the Effect of Substituent Type Connected to N-Atom. *Energy* **2018**, *144*, 1064–1072.
- (46) Cox, M. F.; Weerasooriya, U. Enhanced Propoxylation of Alcohols and Alcohol Ethoxylates. *J. Surfactants Deterg.* **1999**, *2* (1), 59–68.

- (47) Bhawna; Pandey, A.; Dhingra, D.; Pandey, S. Can Common Liquid Polymers and Surfactants Capture CO<sub>2</sub>? *J. Mol. Liq.* **2019**, *277*, 594–605.
- (48) Hans Reich's Collection. NMR Spectroscopy. Data Organic Chemistry. <https://organicchemistrydata.org/hansreich/resources/nmr/?page=06-cmr-03-shift-effects/> (accessed 2024-02-07).
- (49) Richner, G.; Puxty, G. Assessing the Chemical Speciation during CO<sub>2</sub> Absorption by Aqueous Amines Using *in Situ* FTIR. *Ind. Eng. Chem. Res.* **2012**, *51* (44), 14317–14324.
- (50) Dostert, K.-H.; O'Brien, C. P.; Mirabella, F.; Ivars-Barceló, F.; Schauermann, S. Adsorption of Acrolein, Propanal, and Allyl Alcohol on Pd(111): A Combined Infrared Reflection–Absorption Spectroscopy and Temperature Programmed Desorption Study. *Phys. Chem. Chem. Phys.* **2016**, *18* (20), 13960–13973.
- (51) Vrancken, N.; Sergeant, S.; Vereecke, G.; Doumen, G.; Holsteyns, F.; Terryn, H.; De Gendt, S.; Xu, X. Superhydrophobic Breakdown of Nanostructured Surfaces Characterized *in Situ* Using ATR–FTIR. *Langmuir* **2017**, *33* (15), 3601–3609.
- (52) Ma, Y.; Yan, W.; Sun, Q.; Liu, X. Raman and Infrared Spectroscopic Quantification of the Carbonate Concentration in K<sub>2</sub>CO<sub>3</sub> Aqueous Solutions with Water as an Internal Standard. *Geosci. Front.* **2021**, *12* (2), 1018–1030.
- (53) Blombach, B.; Takors, R. CO<sub>2</sub> – Intrinsic Product, Essential Substrate, and Regulatory Trigger of Microbial and Mammalian Production Processes. *Front. bioeng. biotechnol.* **2015**, *3*, 108.
- (54) Yeh, J. T.; Resnik, K. P.; Rygle, K.; Pennline, H. W. Semi-Batch Absorption and Regeneration Studies for CO<sub>2</sub> Capture by Aqueous Ammonia. *Fuel Process. Technol.* **2005**, *86* (14–15), 1533–1546.
- (55) Zhu, K.; Lu, H.; Liu, C.; Wu, K.; Jiang, W.; Cheng, J.; Tang, S.; Yue, H.; Liu, Y.; Liang, B. Investigation on the Phase-Change Absorbent System MEA + Solvent A (SA) + H<sub>2</sub>O Used for the CO<sub>2</sub> Capture from Flue Gas. *Ind. Eng. Chem. Res.* **2019**, *58* (9), 3811–3821.
- (56) Saeed, I. M.; Lee, V. S.; Mazari, S. A.; Si Ali, B.; Basirun, W. J.; Asghar, A.; Ghalib, L.; Jan, B. M. Thermal Degradation of Aqueous 2-Aminoethylethanolamine in CO<sub>2</sub> Capture; Identification of Degradation Products, Reaction Mechanisms and Computational Studies. *Chem. Cent. J.* **2017**, *11* (1), 10.